

Determination of the Chemical Bonding of Ionic Lithium and Proton Exchange in Spinel-Type Manganese Oxides

Yang-Soo Kim,* Hirofumi Kanoh,[†] Takahiro Hirotsu, and Kenta Ooi*

National Institute of Advanced Industrial Science and Technology, 2217-14 Hayashi-cho, Takamatsu 761-0395

[†]Department of Chemistry, Faculty of Science, Chiba University, 1-33 Yayoi, Inage, Chiba 263-8522

(Received April 25, 2001)

A study of the electronic structure and chemical bonding of the Li ions and protons inserted in manganese oxides was performed by a first-principles molecular-orbital method using model clusters ($\text{Mn}_{28}\text{O}_{40}$)³²⁺ for $\lambda\text{-MnO}_2$ and ($\text{X}_5\text{Mn}_{12}\text{O}_{40}$)^{*n*−} for XMn_2O_4 ($n = 31$ ($\text{X} = \text{H}$) and $n = 33$ ($\text{X} = \text{Li}$)). The discrete-variational (DV)-X α method was employed and Mulliken's population analyses were carried out. Strong covalent interactions operate between Mn and O ions in the manganese oxides. Li and hydrogen in manganese oxides are highly ionized. These results are likely to be a very important factor in determining the excellent selectivity of spinel-type manganese oxides for Li⁺ ions and the exchange between Li⁺ and protons.

Spinel-type lithium manganese oxides are characterized by excellent selectivity for Li⁺ ions after topotactic extraction of Li⁺ with an acid.^{1–9} This property makes the materials practical as Li⁺ adsorbents,^{1–6} cathodes for lithium batteries^{11–13} and electrodes for the selective electroinsertion of Li⁺.¹³ Furthermore, the Li⁺ insertion/extraction reaction occurs reversibly, while maintaining the host structure. These characteristics strongly indicate that lithium exists in spinel-type lithium manganese oxides in a highly ionized state. Band-structure calculations of LiMn_2O_4 by first-principles using the LAPW¹⁴ and ab initio pseudopotential methods¹⁵ have been reported. Miura et al.¹⁶ explained the intercalation voltage of $\text{Li}_x\text{Mn}_2\text{O}_4$ using the discrete variational X α (DV-X α) method. Their interest focused on the average intercalation voltage for a lithium-ion battery.

We have studied the mechanism of lithium-ion extraction/insertion reactions with spinel-type lithium manganese oxides in aqueous phases.¹⁷ There are two types of extraction/insertion reactions: a redox-type and an ion-exchange type. Much interest has been focused on spinel-type manganese oxides because they exhibit both redox-type and ion-exchange-type reactions while having the same spinel structure. The extraction of lithium from these materials progresses mainly by the ion-exchange of Li⁺ for protons to give spinel-type manganese oxides with lattice protons.¹⁷ To formulate guiding principles for the mechanism of lithium-ion extraction/insertion reactions

with spinel-type lithium manganese oxides in the aqueous phases, fundamental knowledge regarding the chemical bonding is essential. This study aimed to achieve an understanding of the chemical bondings accompanying by Li⁺ and proton insertions into $\lambda\text{-MnO}_2$ based on the DV-X α molecular-orbital method using a linear combination of atomic orbitals (LCAO) method.

First, we describe the electronic structures of relevant cluster models. Then, the bonding natures of these compounds are discussed through Mulliken's population analysis method¹⁸ in order to elucidate the reason for the selectivity for Li⁺ ions and protons.

Computational Procedures

First-principles molecular orbital (MO) calculations by the DV-X α method^{19, 20} using the program code SCAT²⁰ were performed in order to obtain the electronic structure and chemical bonding of Li and hydrogen inserted into manganese oxides. Numerical atomic orbitals (NAO) were employed as the basis functions. They were generated and optimized by solving the radial part of the Schrödinger equation for a given environment at each iteration of the self-consistent calculation. All of the elements of the Hamiltonian and overlap matrices were calculated numerically based on a discrete variational integration scheme.^{19, 20} The detailed computational procedure has been described in the literature.²⁰ The lattice constants used in the

Table 1. Lattice Constants, Major Interatomic Distances Used for the Calculations and the Calculated Values of Ionicity.

	Lattice parameter/Å	Interatomic distance/Å			Ionicity		
		$d_{\text{Mn-O}}$	$d_{\text{Li-O}}$	$d_{\text{H-O}}$	Mn	O	Li or H
$\lambda\text{-MnO}_2$ ²¹	8.04	1.897	—	—	1.44	−0.77	—
LiMn_2O_4 ²³	8.24	1.944	1.998	—	1.8	−0.96	0.77
HMn_2O_4 ²²	8.04	1.897	—	1.9479	1.95	−0.92	0.52

present study were $a = 8.04 \text{ \AA}$ for $\lambda\text{-MnO}_2$ ²¹ and HMn_2O_4 ,²² and $a = 8.24 \text{ \AA}$ for LiMn_2O_4 ,²³ as given in Table 1. Calculations were made for $\lambda\text{-MnO}_2$, LiMn_2O_4 and HMn_2O_4 using model clusters of $(\text{Mn}_{28}\text{O}_{40})^{32+}$, $(\text{Li}_5\text{Mn}_{12}\text{O}_{40})^{33-}$, and $(\text{H}_5\text{Mn}_{12}\text{O}_{40})^{31-}$ respectively, as shown in Fig. 1. They were cut from real crystals and embedded in a Madelung potential generated by point charges located at the external atomic sites. The atomic orbitals used in the present study were 1s, 1s-2p, 1s-4p, and 1s-2p for H, Li, Mn, and O, respectively.

Results and Discussion

Figure 2 shows the calculated density of states (DOS) of $\lambda\text{-MnO}_2$. The molecular orbital calculation yields discrete molecular orbital (MO) levels. The discrete MO levels are convoluted by Gaussian functions with a full width at half maximum (FWHM) of 1.0 eV for easy visualization of DOS. The energy scale is shifted to make the Fermi level (E_F) zero. In Fig. 2, the partial density of states (PDOS) is also plotted for each atomic orbital. The valence state is constructed principally of the O-

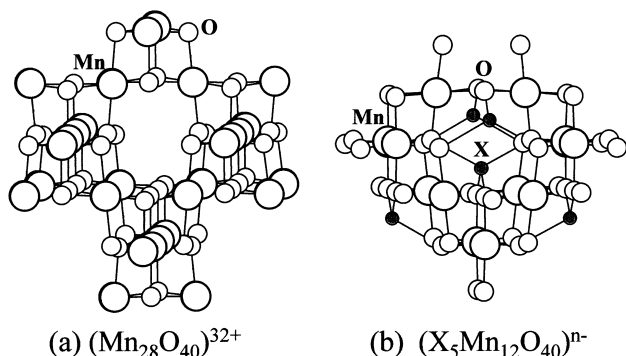


Fig. 1. Cluster models for $\lambda\text{-MnO}_2$ (a) and XMn_2O_4 (X = H or Li) (b).

2s band at -20 eV to -17 eV and the O-2p band at -7 eV to -2 eV . However, these bands also contain components of the Mn-3d and 4sp orbitals, indicating the presence of strong Mn-O covalent bonding in $\lambda\text{-MnO}_2$. The Mn 3d band is located intensively around E_F . A band mainly composed of Mn-4sp orbitals appears in the energy range of more than 12 eV above the Fermi energy. The Mn 3d band also superposes considerably on the O 2p band in the 0–5 eV energy range, making antibonding interactions for Mn-O bonds. A similar bonding characteristic was also found to exist between Ti and S ions in an intercalation compound, TiS_2 in our previous study.²⁵

When Li is inserted (Fig. 3), the filled band located in the energy range from -3 eV to -8 eV remains composed mainly of O-2p orbitals. The partially filled band located around the Fermi energy is also composed mainly of Mn-3d orbitals. An unoccupied band above 10 eV is made of Li-2sp and Mn-4sp orbitals. The Li-2sp states made very slight contributions to the valence band, suggesting that Li is highly ionized in LiMn_2O_4 . On the other hand, the Mn-3d, 4s and 4p bands significantly overlap the O-2p band. The mixing of O-2p states with the Mn 3d band is also notable. Accordingly, there are strong covalent interactions between Mn and O ions, while highly ionized Li atoms make slight covalent interactions with the surrounding atoms. The calculated result agrees well with the experimental result, which has already been reported by the same authors.²⁶ The size of the present clusters is thus sufficient to describe the DOS features.

The formal charges for Mn and O of $\lambda\text{-MnO}_2$ are +4 and -2 , respectively. However, according to Mulliken's population analysis, the effective charges are estimated to be +1.44 for Mn and -0.77 for O, which deviate largely from the formal charges, reflecting the strong covalency between them. When Li is inserted into $\lambda\text{-MnO}_2$, the effective charge of Li is +0.77, as might be expected from its very small electronegativity. The ionicity of O changes from -0.77 to -0.96 , whereas the

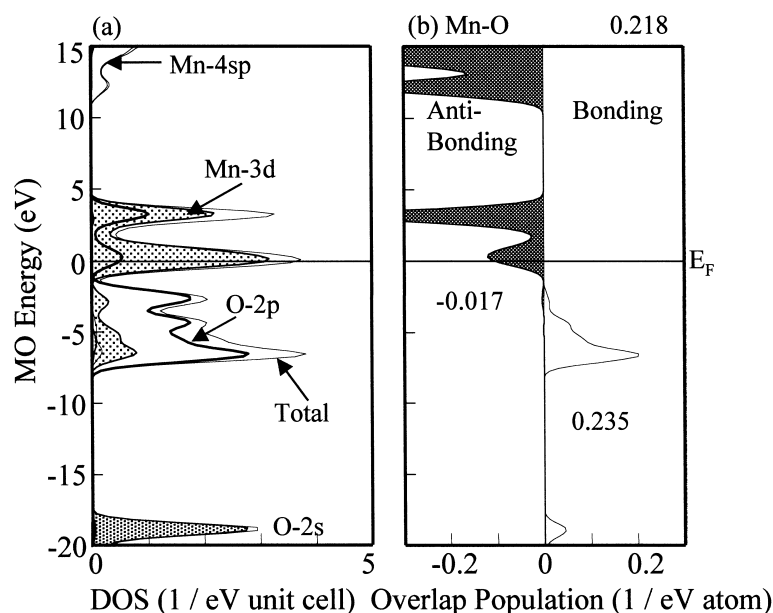


Fig. 2. The total and partial density of states (a) and the overlap population diagram of Mn-O bonds (b) for the $(\text{Mn}_{28}\text{O}_{40})^{32+}$ cluster.

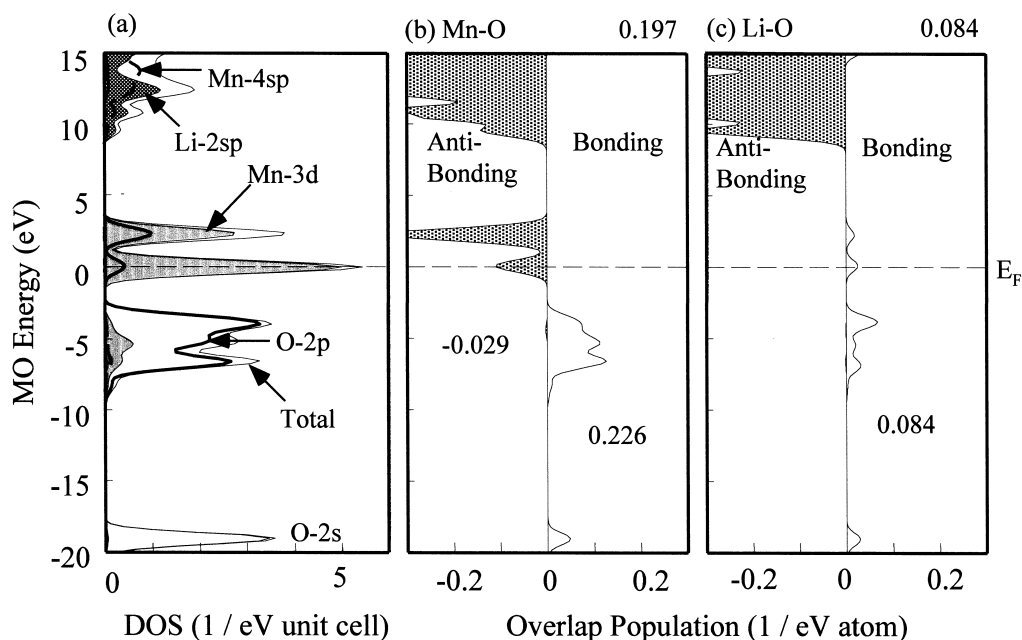


Fig. 3. The total and partial density of states (a) and the overlap population diagrams of Mn–O (b) and Li–O bonds (c) for the $(\text{Li}_5\text{Mn}_{12}\text{O}_{40})^{33-}$ cluster.

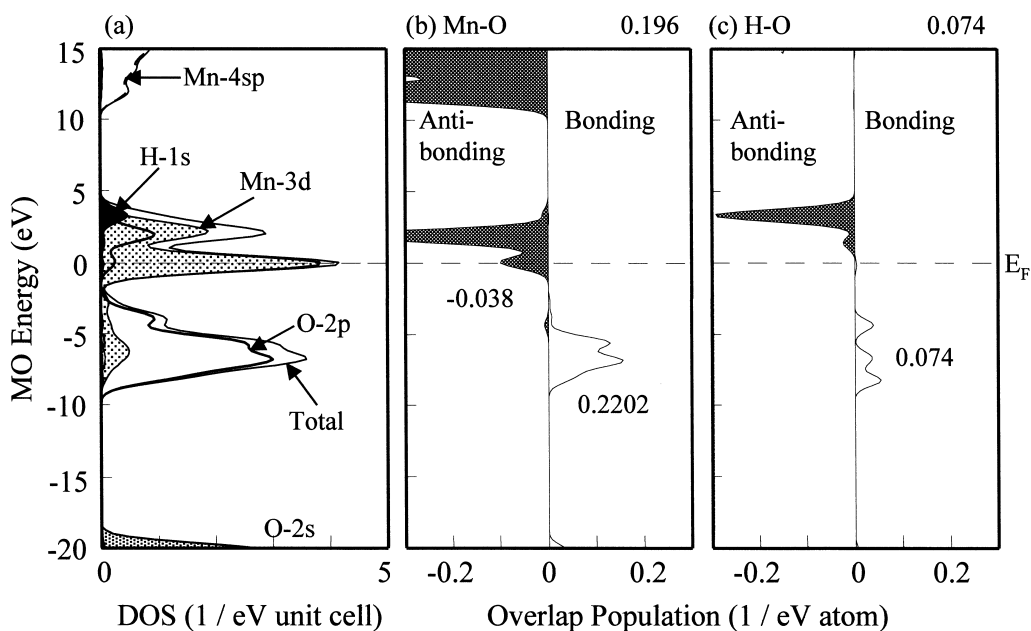


Fig. 4. The total and partial density of states (a) and the overlap population diagrams of Mn–O (b) and H–O bonds (c) for the $(\text{H}_5\text{Mn}_{12}\text{O}_{40})^{31-}$ cluster.

ionicity of Mn changes from +1.44 to +1.8. The formal charge of Mn should change from +4 to +3.5 with lithium insertion, because the formal valence of oxygen is always fixed as -2 in conventional (formal) textbooks, based on a classical view of the charge neutrality in $\lambda\text{-MnO}_2$ and LiMn_2O_4 . However, it should be noted that oxygen ions in lithium-extracted $\lambda\text{-MnO}_2$ are not fully reduced to -2.0 . These results indicate that a charge transfer occurs mainly between lithium and oxygen ions in lithium-inserted compounds. The electronegativity should play a major role in the charge transfer of LiMn_2O_4 .

Such a charge transfer has been reported based on first-principles molecular orbital (MO) calculations^{27, 28} for LiT_mO_2 and T_mO_2 (T_m = transition metal) with a special focus on the changes of chemical bonding by deintercalation. In these cases, the removal of Li was found to cause a significant increase in the intercalation between T_m and O, leading to the oxidation associated with the deintercalation not on T_m but on O. As a result, the net charge of oxygen decreased.

When Li atoms are tentatively replaced by hydrogen (Fig. 4), the filled band located from -3 eV to -10 eV remains

composed mainly of O-2p orbitals. The partially filled band located around the Fermi energy is also composed mainly of Mn-3d, O-2p, and H-1s orbitals. The unoccupied band above 10 eV is made up of Mn-4sp orbitals. H-1s states give a very slight contribution to the valence band, suggesting that hydrogen is highly ionized in HMn_2O_4 . The mixing of O-2p states with the Mn 3d band is also notable. Accordingly, we can conclude that there are strong covalent interactions between Mn and O ions. This suggests that the hydrogen in HMn_2O_4 is in a highly ionized state, and makes only slight covalent interactions with the surrounding atoms. The ion-exchange between lithium ions and protons, therefore, do not significantly affect the valence states of the clusters.

In order to discuss the covalent interactions in more detail, overlap population diagrams for the Mn–O, Li–O and H–O bonds were plotted, as shown in Figs. 2, 3, and 4. The strength of the covalent bonding between atoms A and B can be estimated from the overlap population, which is evaluated as having an energy distribution of overlap population (Q'_{AB}), called the overlap population diagram or COOP (crystal orbital overlap population) diagram. Thus, the bond overlap population (Q_{AB}) between A and B is obtained by summing the Q'_{AB} for all MO levels below E_F . Figs. 2(b), 3(b, c) and 4(b, c) show the bonding and antibonding contributions to the overlap population between Mn and O ions, Li and O ions and H and O ions. The sum of these two components is shown in the upper-right side of each figure. As qualitatively discussed, Figs. 2(b), 3(b), and 4(b) clearly demonstrate strong covalent bonding between Mn and O, and much smaller covalency in the Li–O (0.084) and H–O bonds (0.074) in Figs. 3(c) and 4(c). The shape of DOS and the overlap population diagram of Mn–O are not significantly changed by the insertion of the Li^+ and protons into $\lambda\text{-MnO}_2$. This means that the nature of the Mn–O bond is hardly affected by the exchange of Li^+ and protons. These results are consistent with the widely accepted picture of Li-inserted compounds, and are likely to be a very important factor in determining the excellent selectivity for Li^+ ions of spinel-type lithium manganese oxides.

Conclusions

The electronic structure and chemical bonding of $\lambda\text{-MnO}_2$, LiMn_2O_4 , and HMn_2O_4 were studied by the DV- $X\alpha$ molecular-orbital method using cluster models of $(\text{Mn}_{28}\text{O}_{40})^{32+}$, $(\text{Li}_5\text{Mn}_{12}\text{O}_{40})^{33-}$ and $(\text{H}_5\text{Mn}_{12}\text{O}_{40})^{31-}$, respectively. Mulliken's population analysis was thoroughly conducted to examine the net charges of atoms as well as the magnitudes of covalent bondings between atoms. We found that strong covalent bonding formed between Mn and O ions, while the Li–O and H–O interactions were highly ionic. These results are likely to be a very important factor in determining the optimum selectivity for Li^+ ions of spinel-type lithium manganese oxides through the exchange of Li^+ and protons in aqueous solutions.

References

- 1 G. V. Leont'eva and L. G. Chikova, *J. Appl. Chem. USSR.*, **61**, 734 (1988).
- 2 X. M. Shen and A. J. Clearfield, *J. Solid State Chem.*, **64**, 270 (1986).
- 3 K. Ooi, Y. Miyai, and S. Katoh, *Sep. Sci. Technol.*, **21**, 755 (1986).
- 4 K. Ooi, Y. Miyai, and S. Katoh, *Sep. Sci. Technol.*, **22**, 1779 (1987).
- 5 K. Ooi, Y. Miyai, and S. Katoh, *Solvent Extr. Ion Exch.*, **5**, 561 (1987).
- 6 K. Ooi, Y. Miyai, S. Katoh, H. Maeda, and M. Abe, *Bull. Chem. Soc. Jpn.*, **61**, 407 (1988).
- 7 K. Ooi, Y. Miyai, S. Katoh, H. Maeda, and M. Abe, *Chem. Lett.*, **1988**, 989.
- 8 K. Ooi, Y. Miyai, S. Katoh, H. Maeda, and M. Abe, *Langmuir*, **5**, 150 (1989).
- 9 K. Ooi, Y. Miyai, S. Katoh, H. Maeda, and M. Abe, *Langmuir*, **6**, 289 (1990).
- 10 M. M. Thackeray, W. I. F. David, P. G. Bruce, and J. B. Goodenough, *Mater. Res. Bull.*, **18**, 461 (1983).
- 11 M. M. Thackeray, P. J. Johnson, L. A. De. Picciotto, W. I. F. David, P. G. Bruce, and J. B. Goodenough, *Mater. Res. Bull.*, **19**, 179 (1984).
- 12 M. H. Rossouw, A. De. Kock, L. A. De. Picciotto, M. M. Thackeray, W. I. F. David, and R. M. Ibberson, *Mater. Res. Bull.*, **25**, 173 (1990).
- 13 H. Kanoh, K. Ooi, Y. Miyai, and S. Katoh, *Langmuir*, **7**, 1841 (1991).
- 14 L. Benco, J.-L. Barras, M. Atannasov, C. A. Daul, and E. Deiss, *Solid State Ionics*, **112**, 255 (1998).
- 15 M. K. Aydinol and G. Ceder, *J. Electrochem. Soc.*, **144**, 3832 (1997).
- 16 K. Miura, A. Yamada, and M. Tanaka, *Electrochim. Acta*, **41**, 249 (1996).
- 17 Q. Feng, Y. Miyai, H. Kanoh, and K. Ooi, *Langmuir*, **8**, 1861 (1992).
- 18 R. S. Mulliken, *J. Chem. Phys.*, **23**, 1833 (1955).
- 19 D. E. Ellis, H. Adachi, and F. W. Averill, *Surf. Sci.*, **58**, 497 (1976).
- 20 H. Adachi, M. Tsukada, and C. Satoko, *J. Phys. Soc. Jpn.*, **45**, 875 (1978).
- 21 Y. Gao, M. N. Richard, and J. R. Dahn, *J. Appl. Phys.*, **80**, 4141 (1996).
- 22 The value of $\lambda\text{-MnO}_2$ was tentatively used for HMn_2O_4 cluster model.
- 23 T. Ohzuku, M. Kitagawa, and T. Hirai, *J. Electrochem. Soc.*, **137**, 769 (1990).
- 24 Y.-S. Kim, M. Mizuno, I. Tanaka, and H. Adachi, *Mater. Trans. JIM*, **39**, 709 (1998).
- 25 Y.-S. Kim, Y. Koyama, I. Tanaka, and H. Adachi, *Jpn. J. Appl. Phys.*, **37**, 6440 (1998).
- 26 Y.-S. Kim, H. Kanoh, R. Chitrakar, T. Hirotsu, and K. Ooi, *Chem. Lett.*, **2000**, 1224.
- 27 Y. Koyama, Y.-S. Kim, I. Tanaka, and H. Adachi, *Jpn. J. Appl. Phys.*, **38**, 2024 (1999).
- 28 Y. Koyama, I. Tanaka, Y.-S. Kim, S. R. Nishitani, and H. Adachi, *Jpn. J. Appl. Phys.*, **38**, 4808 (1999).